Author Manuscript

Author Manuscript

Author Manuscript

Author Manuscript

HHS Public Access

Author manuscript

Oncogene. Author manuscript; available in PMC 2018 March 04.

Published in final edited form as:

Oncogene. 2017 December 14; 36(50): 6919–6928. doi:10.1038/onc.2017.305.

A regulatory circuit composed of DNA methyltransferases and receptor tyrosine kinases controls lung cancer cell aggressiveness

Fei Yan[1,#], **Na Shen**[1,#], **Jiuxia Pang**[1], **Na Zhao**[1], **Bo Deng**[2], **Bing Li**[3], **Yanan Yang**[2], **Ping Yang**[2], **Julian R. Molina**[4], and **Shujun Liu**[1,*]

[1]The Hormel Institute, University of Minnesota, 801 16th Avenue NE, Austin, MN 55912, USA

[2]Division of Epidemiology, Mayo Clinic, 200 1st Street SW, Rochester, MN 55905, USA

[3]Department of Microbiology and Immunology, University of Louisville, Louisville, KY 40202, USA

[4]Department of Medical Oncology, Mayo Clinic, 200 1st Street SW, Rochester, MN 55905, USA

Abstract

Overexpression of DNMT1 and KIT is prevalent in lung cancer, yet the underlying molecular mechanisms are poorly understood. While the deregulated activation of DNMT1 or KIT has been implicated in lung cancer pathogenesis, whether and how DNMT1 and KIT orchestrate lung tumorigenesis are unclear. Here, using human lung cancer tissue microarrays and fresh frozen tissues, we found that the overexpression of *DNMT1* is positively correlated with the upregulation of *KIT* in tumor tissues. We demonstrated that *DNMT1* and *KIT* form a positive regulatory loop, in which ectopic *DNMT1* expression increases, whereas targeted *DNMT1* depletion abrogates, KIT signaling cascade through Sp1/*miR-29b* network. Conversely, an increase of *KIT* levels augments, but a reduction of *KIT* expression ablates, *DNMT1* transcription by STAT3 pathway leading to in-parallel modification of the DNA methylation profiles. We provided evidence that KIT inactivation induces global DNA hypomethylation, restores the expression of tumor suppressor $p15^{INK4B}$ through promoter demethylation; in turn, DNMT1 dysfunction impairs KIT kinase signaling. Functionally, *KIT* and *DNMT1* co-expression promotes, whereas dual inactivation of them suppresses, lung cancer cell proliferation and metastatic growth *in vitro* and *in vivo*, in a synergistic manner. These findings demonstrate the regulatory and functional interplay between DNA methylation and tyrosine kinase signaling in propelling tumorigenesis, providing a widely applicable approach for targeting lung cancer.

Users may view, print, copy, and download text and data-mine the content in such documents, for the purposes of academic research, subject always to the full Conditions of use: http://www.nature.com/authors/editorial_policies/license.html#terms

*Correspondence: Shujun Liu, The Hormel Institute, University of Minnesota, 801 16th Avenue NE, Austin, MN 55912, USA. Phone: 507.437.9613; Fax: 507.437.9606; sliu@umn.edu.

#These authors contributed equally to this work

Authors' Contributions: S.J.L. designed the research; F.Y., N.S., J.X.P., N.Z. and B.D. performed research; Y.N.Y., P.Y. and J.R.M. provided the patient samples; F.Y., B.L., P.Y., J.R.M. and S.J.L. analyzed data and wrote the paper; S.J.L. conceived the idea and supervised the whole project. All authors discussed the results and commented on the manuscript.

Competing Interests: The authors state no conflict of interest.

Supplementary Information accompanies the paper on the Oncogene website (http://www.nature.com/onc)

Author Manuscript Author Manuscript Author Manuscript Author Manuscript

Introduction

Lung cancer, an extremely heterogeneous group of human malignancies, is a multi-step process involving genetic (e.g., tyrosine kinase mutations) and epigenetic (e.g., DNA methylation) alterations. DNA methylation takes place mainly at the C5 position of cytosines within CpG dinucleotides and is catalyzed by DNA methyltransferases (DNMTs). It is typically believed that DNMT3a and DNMT3b are *de novo* methyltransferases that newly methylate cytosines[1], but DNMT1 is a maintenance DNMT that is responsible for transferring DNA methylation patterning from parental to daughter cells at cell division.[2, 3] However, certain findings reveal that DNMT1 is also an active *de novo* methyltransferase that cell cycle-independently initiates CpG methylation in cancer cells.[2, 4, 5] In accordance, ectopic *DNMT1* expression leads to genome-wide DNA hypermethylation,[6, 7] whereas genetic or pharmacological inhibition of *DNMT1* expression leads to DNA hypomethylation and the reexpression of epigenetically-silenced tumor suppressor genes (TSGs) coupled by cell cycle arrest, apoptosis and differentiation.[8-10]

The prevalent upregulation of *DNMTs*, particularly *DNMT1*, strongly associates with shorter survival and serves as an independent prognostic factor in lung cancer.[11-13] Mechanistically, *DNMT1* overexpression silences TSGs through promoter DNA hypermethylation, thus conferring a survival advantage to lung cancer cells. A few studies show that multiple factors controlling *DNMT1* gene are increased during cell division and *DNMT1* levels reach a maximum during S phase, suggesting a cell cycle-dependent *DNMT1* regulation.[14-16] However, these findings are insufficient to explain why *DNMT1* was highly expressed in quiescent lung cancer cells and nuclear run-on assays failed to detect obvious change in DNMT1 transcriptional activity throughout the cell cycle. Given that many cells (e.g., cancer stem cells) in lung tumors are quiescent and/or slow-dividing, we propose that cell cycle-independent regulation of *DNMT1* gene is indispensable in lung tumorigenesis.

Constitutively active receptor tyrosine kinases (RTKs) are usually detected in lung cancer patients.[17, 18] The hyperactive KIT, a class III RTK family member, could result from both gene mutations and overamplification, but the relatively low incidence of *KIT* mutations suggests its overamplification to be more essential for lung cancer pathogenesis. In fact, *KIT* overexpression has been documented in the development, progression and drug resistance of lung cancer and survival in some patient subpopulations.[17-21] Inhibitors (e.g., PKC412) for aberrant KIT signaling have been tested in various preclinical and clinical models,[22-26] but they did not bring long-lasting benefits. Given that inhibitor-associated gene overamplification is a frequent event,[19, 27-29] focusing on *KIT* gene regulation could gain better understanding of lung cancer molecular biology and subsequently develop more efficient cancer therapies.

While, as independent entities, the roles of epigenetic dysregulation and hyperactive tyrosine kinases in lung cancer have been studied to a certain extent, the reciprocal gene regulations and functional cooperation between these oncogenic pathways remain elusive. This study aims to test the hypothesis that DNA methylation machinery and KIT kinase signaling may cooperatively regulate lung tumor aggressiveness. That is, KIT kinase may partially

Author Manuscript Author Manuscript Author Manuscript Author Manuscript

transform cells by fostering epigenetic silencing of TSGs. Likewise, through induction of kinase hyperactivity, DNMT1 may facilitate its own persistent activation in cancer cells. We report here that, in lung cancer cells, *DNMT1* and *KIT* form a regulatory circuit consisting of KIT, Sp1/*miR-29b*, STAT3 and DNMT1, whose intercommunication promotes lung tumorigenesis. Dual-genetic and dual-pharmacological inhibition of DNMT1 and KIT leads to a more profound inhibition of tumor cell growth *in vitro* and *in vivo*. These findings support that the DNMT1-KIT loop is a promising therapeutic target in lung cancer.

Results

DNMT1 upregulation is positively correlated with *KIT* overexpression in lung cancer cells

To determine whether expression of DNMTs and KIT is upregulated in lung cancer, human NSCLC TMAs were immunostained using anti-DNMTs and anti-KIT, and the target levels were quantified using H-scores.[29] Representative images are shown in Figure 1a and Supplementary Figure S1a. Compared to the normal adjacent tissues, the tumor tissues displayed higher levels of KIT (53%), DNMT1 (69%), DNMT3a (71%) and DNMT3b (71%) (Supplementary Figure S1b), consistent with the previous reports.[11, 12, 21, 30] When correlated the gene levels with disease stages, H-scores for DNMTs and KIT were significantly higher in later stage (Figure 1b and Supplementary Figure S1c). Importantly, higher levels of KIT were accompanied by DNMT overexpression, but lower KIT expression was observed in tumor tissues carrying lower DNMTs (Figure 1c and Supplementary Figure S1d), indicating a positive correlation between these variables. In support of DNMT1 abundance in DNA methylation, DNMT1 and 5mC levels displayed an in-parallel correlation in tumor tissues (Figure 1d). Although KIT is positively related to all three DNMTs, we mainly focused on DNMT1, because DNMT1 carries both maintenance and *de novo* DNA methylation activity, and its levels serve as an independent prognostic factor in NSCLC.[12, 13] To this end, we assessed *DNMT1* and *KIT* RNA expression in fresh-frozen NSCLC (never smoker) and matched adjacent non-tumor lung tissues (n=30) and in 10 lung cancer cell lines. In agreement with IHC staining results, *DNMT1* and *KIT* was 2.3±0.8 and 5.7±0.5 fold higher, respectively, in tumors than normal tissues (Figure 1e). All tested cell lines displayed higher *KIT* and *DNMT1* expression compared to normal fibroblast MRC-5 (Figure 1f). In line with this, DNMT1 and KIT protein levels were 2.4-fold and 2.7-fold higher, respectively, in fresh-frozen lung tumors than their adjacent normal control (n=7) (Supplementary Figure S1e and 1f). The correlation analysis revealed that DNMT1 and KIT mRNA expression was positively associated in 30 pairs of patient samples (Figure 1g) and 10 cell lines (Figure 1h), but their protein levels exhibited a trend toward positive correlation in patient tissues (n=7, Supplementary Figure S1g). These results support the regulatory and functional interactions between DNMT1 and KIT in lung cancer cells.

DNMT1 upregulates *KIT* through Sp1/*miR-29b* network

Given the positive correlations of DNMT1 and KIT expression in lung cancer cells, we proposed the existence of a regulatory loop between DNA methylation and KIT signaling, in which KIT activity controls the expression of *DNMT1*, whose alteration modifies *KIT* transcription in parallel. To test this, *DNMT1* was knocked down in NSCLC H1299

Author Manuscript Author Manuscript Author Manuscript Author Manuscript

(carcinoma) and H1975 (adenocarcinoma) cells by a Smart siRNA pool containing 4 specific siRNAs or the shRNA3 that showed the most *DNMT1* reduction (>80%, Supplementary Figure S2a). *DNMT1* depletion significantly decreased global DNA methylation (Supplementary Figure S2b) and KIT expression followed by the dephosphorylation of AKT (Figure 2a), a KIT downstream effector.[31] In contrast, enforced *DNMT1* expression resulted in the increased DNA methylation (Supplementary Figure S2c) and the upregulation of KIT coupled by AKT hyperphosphorylation (Figure 2b). Because p53 function is impaired in H1975 (p53 mutation) and H1299 (p53 null) cells, to address if KIT signaling in the context DNMT1 involves p53 function, we manipulated *DNMT1* in NSCLC A549 cells (wild-type p53), and independently verified the findings from H1975 and H1299 cells (Supplementary Figure S2d), supporting a limited role of p53 in DNMT1-related *KIT* expression. Finally, we tested whether DNMT1 regulates additional kinases, such as KRAS, EGFR and MET that are important for lung tumorigenesis, and found that *DNMT1* ablation impaired expression of these three kinases (Supplementary Figure S2e). Collectively, DNMT1 is a positive regulator for tyrosine kinases in lung cancer.

To elucidate how DNMT1 regulates the *KIT* gene, we focused on the Sp1/*miR-29b* network, because Sp1/*miR-29b* has been shown to regulate *KIT* transcription in leukemia,[31] and *miR-29b* was silenced in lung cancer.[11] First, quantification of IHC-stained TMAs revealed Sp1 overexpression in tumor versus normal tissues with the highest levels in stage III disease (Figure 2c and Supplementary Figure S2f). Second, Sp1 and DNMT1 expression in tumors showed a positive association (Supplementary Figure S2g, left). Third, *DNMT1* abrogation reduced (Figure 2d, left), whereas its overexpression increased (Figure 2d, right), the levels of Sp1 and KIT, supporting DNMT1 as a positive Sp1 regulator. Moreover, *Sp1* depletion impaired expression of KIT and DNMTs (Figure 2e). Given a positive correlation of Sp1 with KIT (Supplementary Figure S2g, right), these findings identified DNMT1-Sp1 axis as *KIT* gene regulator. Fourth, to understand how DNMT1 regulates Sp1, we initially examined if DNMT1 regulates *miR-29b*, a Sp1 repressor,[8, 31] and found that *miR-29b* expression was restored upon DNMT1 inactivation (Figure 2f, left). As no CpG islands were identified in *miR-29b* promoter (not shown), *miR-29b* upregulation might occur in a DNA methylation-independent manner through DNMT1-associated NFκB or c-Myc, the reported *miR-29b* suppressors.[31, 32] Indeed, similar to overexpression of wild-type *DNMT1*, enforced expression of catalytically inactive *DNMT1* did not rescue *miR-29b* suppression (Figure 2f, right). Further, *DNMT1* knockdown disrupted the physical interaction of DNMT1 with NFκB or DNMT1 with c-Myc (Figure 2g), which is crucial for their transcriptional activities. Finally, *miR-29b* induction abolished Sp1 and KIT expression (Figure 2h; Supplementary Figure S2h), where DNMT3a and DNMT3b were used as positive controls, and attenuated DNMT1-induced Sp1 upregulation (Figure 2i), supporting that DNMT1 upregulates Sp1 through *miR-29b* suppression. Based on these, we conclude that *KIT* gene is governed by a DNMT1-Sp1/*miR-29b* cascade.

Tyrosine kinases positively regulate DNA methylation

To explore the contribution of KIT to DNA methylation, we initially knocked down *KIT* by siRNA in H1975 and H1299 cells and observed AKT dephosphorylation (Supplementary Figure S3a) coupled by a remarkable DNMT downregulation (Figure 3a). This was verified

Author Manuscript Author Manuscript Author Manuscript Author Manuscript

by the results from shRNA-triggered *KIT* depletion (Supplementary Figure S3b). In contrast, *KIT* overexpression upregulated *DNMT1* gene (Figure 3b). Consistent with the role of Sp1/*miR-29b* in *KIT* and *DNMT1* regulation,[9, 31] enforced *KIT* expression increased, but *KIT* knockdown suppressed, Sp1 expression (Supplementary Figure S3c), which was in contrast to the change of *miR-29b* levels (Supplementary Figure S3d). Consequently, targeted *KIT* depletion decreased (Figure 3c, left; Supplementary Figure S3e), whereas ectopic *KIT* expression increased (Figure 3c, right), global DNA methylation, in line with the positive correlation of KIT with 5mC levels in lung tumors (Supplementary Figure S3f). Notably, while DNMT1 is classically believed to be cell cycle-related enzyme,[2, 3] we did not see obvious changes in cell cycle in cells with *KIT* knockdown or overexpression (not shown). This supports the notion that the alterations of DNMT1-dependent DNA methylation via *KIT* manipulation occur in a cell cycle-independent manner and really reflect the changes of DNMT1 gene abundance or/and enzymatic activity.

Because TSGs are known to be silenced by promoter DNA hypermethylation in NSCLC, we used $p15^{INK4B}$, an inhibitor of cyclin-dependent kinases (INK) that plays a critical role in growth inhibition and cell differentiation, as readout to determine whether kinases regulate TSG $p15^{INK4B}$. qPCR revealed that *KIT* knockdown restored, but *KIT* overexpression further silenced, $p15^{INK4B}$ expression (Figure 3d). Using bisulfite sequencing, we checked the methylation status of $p15^{INK4B}$ promoter (-4 to +535) in H1975 cells. Because +221 to +535 region was barely methylated (Supplementary Figure S3g), we focused on the region from -4 to +247. *KIT* depletion reduced $p15^{INK4B}$ promoter DNA methylation from 11% to 4%, but *KIT* overexpression increased it from 12% to 19% (Figure 3e). Finally, depletion of *KRAS*, *EGFR* and *MET* by their respective shRNAs (Supplementary Figure S3h) led to STAT3 dephosphorylation with a concurrent DNMT1 downregulation and DNA demethylation (Supplementary Figure S3i). Together, the tyrosine kinases serve as unconventional DNA methylation regulators in lung cancer.

STAT3 activity is responsible for KIT-driven *DNMT1* upregulation

To understand how KIT regulates *DNMT1* gene, we decided to target STAT3 signaling, because KIT significantly regulates STAT3 phosphorylation.[33] Once phosphorylated, STAT3 binds specific DNA elements regulating target expression.[34] Given the existence of STAT3 binding elements in *DNMT1* gene promoter, we proposed that *DNMT1* expression in lung cancer cells is, at least partially, governed by the KIT-STAT3 axis. Indeed, *KIT* depletion decreased STAT3 phosphorylation in H1975 and H1299 cells (Supplementary Figure S3j). *STAT3* overexpression enhanced (Figure 3F, right), whereas *STAT3* dephosphorylation by siRNA (Figure 3F, left), shRNA (Supplementary Figure S3k) or its selective inhibitor NSC74859 (Figure 3G) remarkably suppressed, DNMT1 expression. Mechanistically, 1) ChIP analysis revealed that enforced *STAT3* expression enhanced, while *STAT3* knockdown diminished, the binding of total- and phospho-STAT3 in *DNMT1* promoter (Figure 3H); 2) reporter assays showed that ectopic *STAT3* expression increased (Figure 3I, left), whereas NSC74859 treatment decreased (Figure 3I, right), the luciferase activities driven by *DNMT1* promoter region containing STAT3 binding elements, supporting that STAT3 binds and transactivates *DNMT1* promoter in lung cancer cells. Finally, STAT3 dephosphorylation by NSC74859 and siRNA/shRNA reduced global DNA methylation (Figure 3J, Supplementary

Author Manuscript Author Manuscript Author Manuscript Author Manuscript

Figure S3l), substantiating the role of STAT3 in *DNMT1* regulation and suggesting STAT3 inactivation as an alternative approach to achieve DNA demethylation. Collectively, STAT3 signaling bridges the gap between KIT and DNMT1-dependent DNA methylation in lung cancer.

DNMT1 and KIT cooperatively modulate lung tumor cell proliferation *in vitro*

The above results demonstrate that *DNMT1* and *KIT* form a positive regulatory circuit in lung cancer cells. Such positive regulation insinuates a likely biological link and cooperative features in controlling tumor cell growth. To clarify as to whether such biological communication of DNMT1 and KIT impacts cancerous lesions, we first assessed the effects of single gene manipulation on lung cancer cells. We found that depletion of *KIT* or *DNMT1* in H1975 cells remarkably decreased colony number and restrained cell migration (Supplementary Figure S4a). Conversely, enforced expression of *KIT* or *DNMT1* enhanced the clonogenic and wound-healing potential (Supplementary Figure S4b), and, in a time-dependent manner, largely increased the rate of cellular proliferation (Supplementary Figure S4c). To rule out the off-target effects, we transfected H1299 cells with individual shRNA targeting three different region of the *DNMT1* or *KIT* gene. As expected, knockdown of *DNMT1* or *KIT* by individual shRNA led to similar phenotypes, including reduction of colony number and impairment of wound-healing capability (Supplementary Figure S4d and e). Importantly, the rescue experiments revealed that overexpression of *DNMT1* cDNA attenuated the inhibition of wound healing mediated by shRNA-triggered *DNMT1* knockdown in H1299 and H1975 cells (Supplementary Figure S4f and g). Together, these results support the notion that, as independent events, the hyperactive DNMT1 or KIT signaling pathway functions as lung cancer promoting factor.

To test the effects of DNMT1 and KIT interaction on tumor cell growth, we transfected H1975 cells with *KIT* or/and *DNMT1* siRNA at suboptimal doses (50 nM). The siRNA co-transfection resulted in a synergistic downregulation of *KIT* and *DNMT1* (Figure 4a and Supplementary Figure S5a), leading to a more profound DNA demethylation (Figure 4b). Functionally, *DNMT1* and *KIT* co-knockdown synergistically decreased colony number (Figure 4c) and attenuated wound healing (Figure 4d). In contrast, co-transfection with *KIT* and *DNMT1* expression vectors resulted in the most robust increase of their protein expression (Figure 4e and Supplementary Figure S5b) and global DNA methylation (Figure 4f) coupled by the higher colony number (Figure 4g) and the enhanced wound-healing potential (Figure 4h). These findings support that DNMT1 and KIT are functionally interactive in regulating cancer cell growth.

The combined expression of *KIT* and *DNMT1* synergistically accelerates lung tumor cell growth and metastasis *in vivo*

To determine if DNMT1 and KIT orchestrate tumor growth, we overexpressed *DNMT1* or/and *KIT* in H1975 cells. About 1×10^6 transfected cells were subcutaneously injected into nude mice and the experiments were terminated at day 28 after engraftment. Compared to single gene, *DNMT1* and *KIT* co-expression had a more potent effect on tumorigenesis, as indicated by the enhanced tumor volume (control, 54±7 mm^3; *DNMT1*, 243±73 mm^3; *KIT*, 231±84 mm^3; *DNMT1* plus *KIT*, 512±127 mm^3) and the increased tumor weight (control,

Author Manuscript Author Manuscript Author Manuscript Author Manuscript

56±6 mg; *DNMT1*, 266±26 mg; *KIT*, 248±25 mg; *DNMT1* plus *KIT*, 465±51 mg) (Figure 5a–c). Moreover, *KIT* and *DNMT1* co-expression led to the largest lesion area (control, 5±2%; *DNMT1*, 36±6%; *KIT*, 42±9%; *DNMT1* plus *KIT*, 85±8%) and the most metastatic foci (control, 1.7±0.5; *DNMT1*, 9.7±1.5; *KIT*, 11.0±3.0; *DNMT1* plus *KIT*, 20.0±4.1) in lungs (Figure 5d and 5e). Histological examination of tumor sections using Ki-67 or H&E staining revealed that the co-expression mice displayed higher levels of tumor proliferation than other groups (Figure 5f). Mechanistic investigation showed that tumor cells from *DNMT1* and *KIT* co-transfection group exhibited the highest levels of *DNMT1*, *KIT* and 5mC with the least levels of *E-cadherin*, a known suppressor of tumor cell invasion and migration (Figure 5f). Altogether, these findings support that *KIT* overexpression communicates with *DNMT1* upregulation to induce more aggressive lung cancer.

Dual inactivation of *KIT* and *DNMT1* leads to synergistic blockage of lung tumorigenesis and pulmonary metastatic growth

While the synergistic effects of *KIT*/*DNMT1* co-expression in nude mice clearly support their functional interplay in lung cancer, the recipient mice are immunodeficient. To this end, we employed the C57BL/6 mouse with competent immune system and LL/2, which is syngeneic to C57BL/6 with lung metastatic potential. We initially transfected LL/2 cells with mouse *DNMT1* or *KIT* siRNA and found, similar to the results from H1975 cells, *DNMT1* depletion impaired KIT expression and phosphorylation; in contrast, *KIT* knockdown decreased DNMT1 expression (Supplementary Figure S6a). We then knocked down both *KIT* and *DNMT1* in LL/2 cells (Supplementary Figure S6b, left and middle) and evidenced a synergistic reduction of global DNA methylation (Supplementary Figure S6b, right), tumor cell migration (Supplementary Figure S6c) and colony number (Supplementary Figure S6d), compared to single gene depletion.

To examine the *in vivo* effects of dual knockdown of DNMT1 and KIT, the transfected LL/2 cells (0.5×10^6) were subcutaneously injected into C57BL/6 mice (n=6 mice/group), which were sacrificed at day 20 post-engraftment. Compared to the mice injected cells with the single agent alone, the mice injected with cells with *DNMT1* and *KIT* co-depletion had the smallest tumor volume (scramble, 585±87 mm^3; *DNMT1*, 260±39 mm^3; *KIT*, 247±31 mm^3; *DNMT1* plus *KIT*, 39±6 mm^3) and the least tumor weight (scramble, 643±80 mg; *DNMT1*, 276±41 mg; *KIT*, 245±28 mg; *DNMT1* plus *KIT*, 123±16 mg) (Figure 6a, 6b and Supplementary Figure S6e) and also displayed the fewest nodules (scramble, 21.2±5.5; *DNMT1*, 11.5±5.4; *KIT*, 10.0±2.6; *DNMT1* plus *KIT*, 1.2±1.2) and the smallest lesion area (scramble, 71±7%; *DNMT1*, 40±8%; *KIT*, 35±11%; *DNMT1* plus *KIT*, 8±5%) in lung (Figure 6c and d). Moreover, as shown in Figure 6e, *KIT*/*DNMT1* co-suppression resulted in the lowest levels of tumor cell proliferation (evident by Ki-67 and H&E staining), suggesting that *KIT*/*DNMT1* co-dysfunction has more robust effects on blocking lung tumorigenesis *in vivo*, which might take place through the synergistic suppression of KIT and DNMT1 oncogenic pathways, as supported by the lowest levels of *KIT*, *DNMT1* and 5mC, and the highest *E-cadherin* expression in co-knockdown group. In agreement with the dual-depletion results, treatment with the combination of decitabine and PKC412 led to more robust inhibition of cell migration in H1975 cells expressing relatively higher level of DNMT1 and KIT, but no obvious changes in cell migration of H1650 cells expressing relatively lower

Author Manuscript Author Manuscript Author Manuscript Author Manuscript

level of them (Supplementary Figure S7), supporting an idea that the double-targeted therapy might be more efficient in NSCLC cells highly expressing both DNMT1 and KIT, which merits systematic investigations. Importantly, such combination approach in tumor-bearing mice achieved greater therapeutic outcomes, as demonstrated by the smallest tumor volume (control, 1559±380 mm^3; PKC412, 855±223 mm^3; decitabine, 894±212 mm^3; decitabine plus PKC412, 431±153 mm^3), the least tumor weight (control, 1865±203 mg; PKC412, 1069±180 mg; decitabine, 992±276 mg; decitabine plus PKC412, 413±102 mg) and the fewest nodules (control, 25±4; PKC412, 12±3; decitabine, 14±4; decitabine plus PKC412, 6±2) in lung (Supplementary Figure S8). Collectively, these findings further strengthen the idea of DNMT1-KIT crosstalk in regulating the invasive and migratory abilities of lung cancer cells.

Discussion

We and others have previously shown that abnormal DNMT or kinase activities are functionally essential for cancer pathogenesis.[8, 31, 35] However, whether and how *DNMT1* and *KIT* genes are reciprocally regulated in cancer cells, and whether and how DNMT1 and KIT deregulation orchestrates cancerous lesions remain intriguing. In the present study, we used lung cancer as readout model and provided a series of evidence underscoring two important concepts. On the one hand, *DNMT1* and *KIT* form a regulatory circuit, in which, KIT positively regulates DNA methylation through STAT3 pathway; in turn, DNMT1 reinforces KIT kinase cascade via Sp1/*miR-29b* network; on the other hand, DNMT1 and KIT functionally cooperate in provoking lung tumorigenesis, and dual inactivation of them results in more robust cancer cell growth inhibition *in vitro* and tumor regression *in vivo*. Thus, DNMT1-KIT vicious circle acts as a key regulator of cell fate decision in cancer pathogenesis representing an attractive target for designing innovative therapeutic strategies.

Our initial motivation in studying aberrant kinase in concert with epigenetic programming in lung cancer came from our previous demonstrations that 1) oncogene abundance, when compared to mutations, could be better therapeutic target;[9, 31] 2) disruption of oncogenic expression abolishes the enzymatic activity, regardless of mutation status; 3) Sp1 and *miR-29b* are involved in the transcriptional regulation of *DNMT1* and *KIT*, respectively.[8, 9, 11, 31] In the present study, we showed that DNMT1 and KIT levels were much higher in lung tumor tissues and cell lines than in normal counterparts. Importantly, KIT expression was positively correlated with DNMT1 expression at both protein and RNA levels, together, leading to our hypothesis that DNMT1 and KIT have regulatory interactions in controlling their cellular levels and functional cooperation in the regulation of cancer cell growth. In fact, modulation of DNMT1 activity positively changed the functions of multiple kinase signaling; conversely, *KIT* expression upregulated *DNMT1* gene leading to an increase of global DNA methylation and further $p15^{INK4B}$ silencing by promoter DNA hypermethylation. In support of this, KIT inactivation decreased the levels of DNMT1 expression and global DNA methylation with a concurrent $p15^{INK4B}$ re-expression through promoter DNA hypomethylation. Functionally, we demonstrated that, as individual events, overexpression of *DNMT1* or *KIT* increased, whereas inhibition of them impaired, lung cancer cell expansion, consistent with previous reports that upregulation of *DNMT1* or *KIT* predicts poor prognosis.[11-13, 20] More importantly, dual-manipulation of DNMT1 and KIT

Author Manuscript Author Manuscript Author Manuscript Author Manuscript

function displayed more robust effects on tumor cell growth *in vitro* and tumorigenesis *in vivo*. Given that EGFR, MET and KRAS positively regulate DNMT1-dependent DNA methylation or *vice versa*, our findings establish a novel mechanistic model describing epigenome-kinome crosstalk in controlling cancer cell survival and proliferation.

It is postulated that *DNMT1* upregulation partially involves the deregulation of miRs (e.g., *miR-29b*)[8] or the disruption of p53/Sp1 interaction.[36] Although AKT1 kinase has also been found to phosphorylate and stabilize DNMT1 protein,[37] a comprehensive characterization of whether and how tyrosine kinases regulate *DNMT1* transcription has not been yet initiated. Our data uncovered KIT functions as additional modulators for, not only specific genomic loci (e.g., $p15^{INK4B}$), but also the global DNA methylation, through *DNMT1* transactivation in lung cancer. In support of this, ectopic *KIT* expression increased the levels of *DNMT1* and DNA methylation, while KIT ablation diminished DNMT1-dependent DNA methylation and restored $p15^{INK4B}$ expression. Mechanistically, we demonstrated that KIT regulates *DNMT1* gene, at least partially, through the STAT3 pathway, because KIT significantly modulates STAT3 functions, whose changes paralleled *DNMT1* levels. Given that DNMT1 can be phosphorylated on multiple sites by kinases, like AKT[37] or PKC isoforms,[38] and as AKT is one of KIT downstream effectors, we can't exclude the possibility that KIT may indirectly phosphorylate and stabilize DNMT1 protein, another latent mechanism controlling KIT-driven DNA hypermethylation. Collectively, these results define KIT as a non-classical epigenetic regulator in lung cancer.

KIT overamplification strongly associates with an aggressive tumor phenotype in lung cancer, but how *KIT* gene is upregulated remains elusive. The positive correlation of *KIT* with *DNMT1* expression in lung cancer cells raises the possibility that *DNMT1* overexpression could be one cause of *KIT* upregulation, which has not yet been demonstrated. We provide compelling evidence that DNMT1 positively regulates *KIT* gene, mechanistically, through Sp1/*miR-29b* loop. Notably, *DNMT1* manipulation positively changed Sp1 levels, but negatively altered *miR-29b* expression. Given that *miR-29b* indirectly suppresses *DNMT1* gene,[8] the current findings complete an DNMT1/*miR-29b* negative loop through Sp1 in lung cancer. Additionally, we previously reported that Sp1 is an upstream regulator of *DNMT1* gene,[9] here we identified DNMT1 as *Sp1* gene activator, thus finalizing Sp1/DNMT1 positive circuit in lung cancer. Although this possibility has not been evaluated, DNMT1 may regulate *KIT* via the alterations of promoter DNA methylation, because Sp1 binding elements (CG-rich region) on *KIT* promoter have been shown to be modified by DNA methylation.[39] Given the multiple CpG islands at *KIT* promoter, it is likely that *KIT* expression is partially attributed to promoter DNA methylation in lung cancer cells, thus raising a question of how Sp1/*miR-29b* network and promoter DNA methylation achieve a balance to ensure that KIT levels meet its cellular functions. The answers to this question are new insights into the cooperative features of epigenome and kinome in cancer biology.

In summary, our results demonstrate a vicious circle between DNMT1 and KIT in determining lung cancer cell fate. Such regulatory and functional cooperation is not restricted to a specific pathway, but possibly extended to the kinome and epigenome. Not only do these findings add a new layer to the complexity of molecular processes regulating

Author Manuscript Author Manuscript Author Manuscript Author Manuscript

cancerous lesions, but also highlight the capability of tyrosine kinases to modulate DNA methylation; in turn, DNA methyltransferases to alter kinase cascades. Given the highly heterogeneous features of lung tumorigenesis, it remains unclear why certain lung cancer subtypes exhibit highly expressed kinases or DNMTs, but not both simultaneously. Further elucidation promises to be informative about the molecular rules governing epigenetic and kinase aberrations.

Materials and Methods

Plasmids and chemicals

STAT3 expression plasmid was constructed by cloning the PCR fragments into the HindIII and XhoI sites of pcDNA4 vector. *KIT* expression plasmid was obtained by inserting *KIT* gene sequence into pBABE-puro retroviral vector. Construction of *DNMT1* luciferase reporter was obtained by subcloning promoter fragment (−1048/+36) containing two STAT3 binding sites (−194/−186: TTTACTCAA and −423/−416: TTAAAAAA) into the KpnI and HindIII sites of pGL3-basic. The catalytically inactive *DNMT1* (C1226W, cysteine to tryptophan) plasmid was generated using a QuikChange XL Site-directed mutagenesis Kit (200521, QuikChange, Agilent Technologies, Santa Clara, CA). Primer sequences are listed in Supplemental table. All constructs were verified by DNA sequencing. The shRNA and scramble vectors for *DNMT1*, *KIT* and *STAT3* were obtained from BMGC RNAi (University of Minnesota). Synthetic *miR-29b* (AS00LRA3) or negative scrambled control (AM17111) were purchased from Ambion. The On-target^{plus} Smart pool siRNAs containing a mixture of 4 oligonucleotides for *KIT* (L-003150), *DNMT1* (L-004605), *Sp1* (L-026959) and their scramble oligos were purchased from GE Healthcare. *STAT3* siRNA and scramble (sequences in Supplemental table) were synthesized by Integrated DNA Technologies. PKC412 (P-7600) and nilotinib (N-8207) were purchased from LC Laboratories (Woburn, MA), decitabine (A3656) and procainamide (P9391) from Sigma-Aldrich (St. Louis, MO), and NSC74859 (S3I-201) from SelleckBio (Houston, TX).

Cell lines and transfections

Cell lines (H1975, H1299, A549, H1650, H520, H460, H441, H358, H69, H82, LL/2 and MRC-5) were obtained from American Type Culture Collection (Manassas, Virginia). LL/2 was cultured in DMEM, human normal lung fibroblast MRC-5 in EMEM and others in RPMI1640 containing 10% fetal bovine serum (FBS, 16140-071, Life Technology, Waltham, MA). Cell lines were newly purchased with no further authentication and no further testing for mycoplasma. The transfection of siRNAs (100 nM), *miR-29b* (100 nM), and expression and shRNA vectors (2 μg) were performed as previously described.[29, 40, 41]

Lung cancer tissue microarray

Lung cancer tissue microarray (TMA) slides were obtained from US Biomax (LC10012, Rockville, MD). The TMAs contain 45 cases of non-small cell lung carcinoma (NSCLC, 26 cases of squamous cell carcinoma, 18 cases of adenosquamous carcinoma, 1 case of large cell carcinoma) at different stages (18 cases of Stage I, 16 cases of Stage II, 10 cases of Stage III and 1 case of Stage IV), and adjacent tissue, 5 normal tissues with duplicate cores per case. The slides were stained with antibodies from Abcam: anti-DNMT1 (ab19905),

Author Manuscript Author Manuscript Author Manuscript Author Manuscript

anti-DNMT3a (ab2850) and anti-DNMT3b (ab13604); Cell Signaling Technology: anti-KIT (3074); Santa Cruz Biotechnology (Dallas, Texas): anti-Sp1 (sc-14027), and quantified as previously described.[29, 41]

Western blot

After the various treatments, the whole cellular lysates were prepared by harvesting the cells in 1×cell lysis buffer.[29, 40, 42] The antibodies used are from Santa Cruz Biotechnology: anti-Sp1 (sc-59) and anti-β-Actin (sc-1616); Cell Signaling Technology: anti-KIT (3392S), anti-phospho-KIT (Tyr719, 3391L), anti-AKT, anti-phospho-AKT (Ser473, 9272), anti-STAT3 (9139), and anti-phospho-STAT3 (Tyr705, 9131); New England Biolabs: anti-DNMT1 (M0231L, Ipswich, MA); EMD Millipore (Billerica, MA): EGFR (04-281); Proteintech: MET (19971-1-AP, Rosemont, IL) and Abcam: anti-KRAS (ab180772).

Chromatin immunoprecipitations (ChIP)

ChIP was performed in H1975 cells transfected with *STAT3* expression, shRNA or control vectors (2 μg) as previously described.[31, 42] The anti-STAT3 (9139) and anti-phospho-STAT3 (Tyr705, 9131) (Cell Signaling Technology) were used.

RNA isolation, cDNA preparation and qPCR

RNA was isolated using miRNAeasy Kit (217004, Qiagen) and cDNA was synthesized by SuperScript® III First-Strand Synthesis System (18080-051, Invitrogen). qPCR was performed by TaqMan (*DNMT1*, *KIT, Sp1*) or SYBR-Green (4309155, $p15^{INK4B}$) master mix, which was normalized by *18S* levels. The primer sequences are listed in Supplemental table. For *miR-29b* expression, qPCR was conducted by TaqMan microRNA assays (4427975) and normalized by U44/48.[31, 41]

In vivo tumor growth and metastasis assays

C57BL/6 and athymic nude mice (male, 4–6 weeks old) were purchased from the Harlan Laboratories. All animal experiments were approved by the University of Minnesota Institutional Animal Care and Use Committee. In co-depletion or co-expression experiments, the transfected LL/2 (0.5×10^6) or H1975 (1×10^6) cells were injected into C57BL/6 or nude mice, respectively. In therapeutic experiments, LL/2 (0.5×10^6) were injected into C57BL/6 mice. Drugs were prepared just prior to administration by dissolving it in ethanol to give a clear solution and diluting with PEG400 and saline (ratio 15:38:47). When the tumor size approached 50 mm^3, the tumor-bearing mice were given by intraperitoneal injection three times per week of 25 mg/kg decitabine or 5 mg/kg PKC412 (suboptimal) as single or in combination form for 2 weeks. Mice were sacrificed at indicated time points and excised lungs were fixed with 10% formaldehyde. The tumors were fixed in 10% neutral buffered formalin for 24 hours at 4°C and transferred to phosphate buffered saline for paraffin embedded blocks. The histopathological examination was performed as previously described.[29, 41]

Author Manuscript Author Manuscript Author Manuscript Author Manuscript

Statistical analysis

The quantification for target changes was performed using the Student's t test. The percentage of comparison between low and high gene expression in TMAs was calculated using the χ^2 test. Correlation data were determined by Pearson correlation coefficients. Differences were considered statistically significant at $P < 0.05$. All P values were determined by unpaired, two-tailed Student's t test (details in Supplementary Methods).

Supplementary Material

Refer to Web version on PubMed Central for supplementary material.

Acknowledgments

This work was supported in part by Hormel Foundation (S. Liu) and National Cancer Institute (Bethesda, MD) grants R01CA149623 (S. Liu) and R21CA155915 (S. Liu).

References

1. Okano M, Bell DW, Haber DA, Li E. DNA methyltransferases Dnmt3a and Dnmt3b are essential for de novo methylation and mammalian development. Cell. 1999; 99:247–257. [PubMed: 10555141]
2. Gowher H, Stockdale CJ, Goyal R, Ferreira H, Owen-Hughes T, Jeltsch A. De novo methylation of nucleosomal DNA by the mammalian Dnmt1 and Dnmt3A DNA methyltransferases. Biochemistry. 2005; 44:9899–9904. [PubMed: 16026162]
3. Yu W, Jin C, Lou X, Han X, Li L, He Y, et al. Global analysis of DNA methylation by Methyl-Capture sequencing reveals epigenetic control of cisplatin resistance in ovarian cancer cell. PloS one. 2011; 6:e29450. [PubMed: 22216282]
4. Arand J, Spieler D, Karius T, Branco MR, Meilinger D, Meissner A, et al. In vivo control of CpG and non-CpG DNA methylation by DNA methyltransferases. PLoS genetics. 2012; 8:e1002750. [PubMed: 22761581]
5. Jeltsch A, Jurkowska RZ. New concepts in DNA methylation. Trends in biochemical sciences. 2014; 39:310–318. [PubMed: 24947342]
6. Bauer C, Gobel K, Nagaraj N, Colantuoni C, Wang M, Muller U, et al. Phosphorylation of TET proteins is regulated via O-GlcNAcylation by the glycosyltransferase OGT. J Biol Chem. 2015
7. Wu J, Issa JP, Herman J, Bassett DE Jr, Nelkin BD, Baylin SB. Expression of an exogenous eukaryotic DNA methyltransferase gene induces transformation of NIH 3T3 cells. Proc Natl Acad Sci U S A. 1993; 90:8891–8895. [PubMed: 8415627]
8. Garzon R, Liu S, Fabbri M, Liu Z, Heaphy CE, Callegari E, et al. MicroRNA -29b induces global DNA hypomethylation and tumor suppressor gene re-expression in acute myeloid leukemia by targeting directly DNMT3A and 3B and indirectly DNMT1. Blood. 2009
9. Liu S, Liu Z, Xie Z, Pang J, Yu J, Lehmann E, et al. Bortezomib induces DNA hypomethylation and silenced gene transcription by interfering with Sp1/NF-kappaB-dependent DNA methyltransferase activity in acute myeloid leukemia. Blood. 2008; 111:2364–2373. [PubMed: 18083845]
10. Miller AA, Pang H, Hodgson L, Ramnath N, Otterson GA, Kelley MJ, et al. A phase II study of dasatinib in patients with chemosensitive relapsed small cell lung cancer (Cancer and Leukemia Group B 30602). Journal of thoracic oncology : official publication of the International Association for the Study of Lung Cancer. 2010; 5:380–384.
11. Fabbri M, Garzon R, Cimmino A, Liu Z, Zanesi N, Callegari E, et al. MicroRNA-29 family reverts aberrant methylation in lung cancer by targeting DNA methyltransferases 3A and 3B. Proc Natl Acad Sci U S A. 2007; 104:15805–15810. [PubMed: 17890317]
12. Lin RK, Hsu HS, Chang JW, Chen CY, Chen JT, Wang YC. Alteration of DNA methyltransferases contributes to 5′CpG methylation and poor prognosis in lung cancer. Lung Cancer. 2007; 55:205–213. [PubMed: 17140695]

Author Manuscript Author Manuscript Author Manuscript Author Manuscript

13. Tamborini E, Bonadiman L, Negri T, Greco A, Staurengo S, Bidoli P, et al. Detection of overexpressed and phosphorylated wild-type kit receptor in surgical specimens of small cell lung cancer. Clin Cancer Res. 2004; 10:8214–8219. [PubMed: 15623596]
14. Litz J, Krystal GW. Imatinib inhibits c-Kit-induced hypoxia-inducible factor-1alpha activity and vascular endothelial growth factor expression in small cell lung cancer cells. Molecular cancer therapeutics. 2006; 5:1415–1422. [PubMed: 16818499]
15. McCabe MT, Davis JN, Day ML. Regulation of DNA methyltransferase 1 by the pRb/E2F1 pathway. Cancer Res. 2005; 65:3624–3632. [PubMed: 15867357]
16. Kimura H, Nakamura T, Ogawa T, Tanaka S, Shiota K. Transcription of mouse DNA methyltransferase 1 (Dnmt1) is regulated by both E2F-Rb-HDAC-dependent and -independent pathways. Nucleic Acids Res. 2003; 31:3101–3113. [PubMed: 12799438]
17. Jafri NF, Ma PC, Maulik G, Salgia R. Mechanisms of metastasis as related to receptor tyrosine kinases in small-cell lung cancer. Journal of environmental pathology, toxicology and oncology : official organ of the International Society for Environmental Toxicology and Cancer. 2003; 22:147–165.
18. Levina V, Marrangoni A, Wang T, Parikh S, Su Y, Herberman R, et al. Elimination of human lung cancer stem cells through targeting of the stem cell factor-c-kit autocrine signaling loop. Cancer Res. 2010; 70:338–346. [PubMed: 20028869]
19. Tsuura Y, Hiraki H, Watanabe K, Igarashi S, Shimamura K, Fukuda T, et al. Preferential localization of c-kit product in tissue mast cells, basal cells of skin, epithelial cells of breast, small cell lung carcinoma and seminoma/dysgerminoma in human: immunohistochemical study on formalin-fixed, paraffin-embedded tissues. Virchows Archiv : an international journal of pathology. 1994; 424:135–141. [PubMed: 7514077]
20. Boldrini L, Ursino S, Gisfredi S, Faviana P, Donati V, Camacci T, et al. Expression and mutational status of c-kit in small-cell lung cancer: prognostic relevance. Clin Cancer Res. 2004; 10:4101–4108. [PubMed: 15217946]
21. Jemal A, Siegel R, Ward E, Murray T, Xu J, Thun MJ. Cancer statistics, 2007. CA: a cancer journal for clinicians. 2007; 57:43–66. [PubMed: 17237035]
22. Carlomagno F, Santoro M. Receptor tyrosine kinases as targets for anticancer therapeutics. Curr Med Chem. 2005; 12:1773–1781. [PubMed: 16029146]
23. Rossi A, Maione P, Colantuoni G, Ferrara C, Rossi E, Guerriero C, et al. Recent developments of targeted therapies in the treatment of non-small cell lung cancer. Curr Drug Discov Technol. 2009; 6:91–102. [PubMed: 19519336]
24. Ansari J, Palmer DH, Rea DW, Hussain SA. Role of tyrosine kinase inhibitors in lung cancer. Anticancer Agents Med Chem. 2009; 9:569–575. [PubMed: 19519298]
25. Monnerat C, Henriksson R, Le Chevalier T, Novello S, Berthaud P, Faivre S, et al. Phase I study of PKC412 (N-benzoyl-staurosporine), a novel oral protein kinase C inhibitor, combined with gemcitabine and cisplatin in patients with non-small-cell lung cancer. Ann Oncol. 2004; 15:316–323. [PubMed: 14760128]
26. Schrump DS, Fischette MR, Nguyen DM, Zhao M, Li X, Kunst TF, et al. Phase I study of decitabine-mediated gene expression in patients with cancers involving the lungs, esophagus, or pleura. Clin Cancer Res. 2006; 12:5777–5785. [PubMed: 17020984]
27. Gauler TC, Christoph DC, Fischer J, Frickhofen N, Huber R, Gonschorek C, et al. Phase-I study of sagopilone in combination with cisplatin in chemotherapy-naive patients with metastasised small-cell lung cancer. Eur J Cancer. 2013
28. Yuan WC, Lee YR, Huang SF, Lin YM, Chen TY, Chung HC, et al. A Cullin3-KLHL20 Ubiquitin ligase-dependent pathway targets PML to potentiate HIF-1 signaling and prostate cancer progression. Cancer Cell. 2011; 20:214–228. [PubMed: 21840486]
29. Yan F, Shen N, Pang J, Molina JR, Yang P, Liu S. The DNA Methyltransferase DNMT1 and Tyrosine-Protein Kinase KIT Cooperatively Promote Resistance to 5-Aza-2′-deoxycytidine (Decitabine) and Midostaurin (PKC412) in Lung Cancer Cells. J Biol Chem. 2015; 290:18480–18494. [PubMed: 26085088]

Author Manuscript Author Manuscript Author Manuscript Author Manuscript

30. Mott JL, Kurita S, Cazanave SC, Bronk SF, Werneburg NW, Fernandez-Zapico ME. Transcriptional suppression of mir-29b-1/mir-29a promoter by c-Myc, hedgehog, and NF-kappaB. Journal of cellular biochemistry. 2010; 110:1155–1164. [PubMed: 20564213]
31. Liu S, Wu LC, Pang J, Santhanam R, Schwind S, Wu YZ, et al. Sp1/NFkappaB/HDAC/miR-29b regulatory network in KIT-driven myeloid leukemia. Cancer Cell. 2010; 17:333–347. [PubMed: 20385359]
32. Li W, Melton DW. Cisplatin regulates the MAPK kinase pathway to induce increased expression of DNA repair gene ERCC1 and increase melanoma chemoresistance. Oncogene. 2012; 31:2412–2422. [PubMed: 21996734]
33. Crivellari G, Monfardini S, Stragliotto S, Marino D, Aversa SM. Increasing chemotherapy in small-cell lung cancer: from dose intensity and density to megadoses. The oncologist. 2007; 12:79–89. [PubMed: 17227903]
34. Abidin AZ, Garassino MC, Califano R, Harle A, Blackhall F. Targeted therapies in small cell lung cancer: a review. Therapeutic advances in medical oncology. 2010; 2:25–37. [PubMed: 21789124]
35. Poirier JT, Gardner EE, Connis N, Moreira AL, de Stanchina E, Hann CL, et al. DNA methylation in small cell lung cancer defines distinct disease subtypes and correlates with high expression of EZH2. Oncogene. 2015; 34:5869–5878. [PubMed: 25746006]
36. Lin RK, Wu CY, Chang JW, Juan LJ, Hsu HS, Chen CY, et al. Dysregulation of p53/Sp1 control leads to DNA methyltransferase-1 overexpression in lung cancer. Cancer Res. 2010; 70:5807–5817. [PubMed: 20570896]
37. Itamochi H, Nishimura M, Oumi N, Kato M, Oishi T, Shimada M, et al. Checkpoint kinase inhibitor AZD7762 overcomes cisplatin resistance in clear cell carcinoma of the ovary. International journal of gynecological cancer : official journal of the International Gynecological Cancer Society. 2014; 24:61–69. [PubMed: 24362713]
38. Liu LZ, Zhou XD, Qian G, Shi X, Fang J, Jiang BH. AKT1 amplification regulates cisplatin resistance in human lung cancer cells through the mammalian target of rapamycin/p70S6K1 pathway. Cancer Res. 2007; 67:6325–6332. [PubMed: 17616691]
39. Schneider BJ, Kalemkerian GP, Ramnath N, Kraut MJ, Wozniak AJ, Worden FP, et al. Phase II trial of imatinib maintenance therapy after irinotecan and cisplatin in patients with c-Kit-positive, extensive-stage small-cell lung cancer. Clinical lung cancer. 2010; 11:223–227. [PubMed: 20630823]
40. Yan F, Shen N, Pang JX, Zhang YW, Rao EY, Bode AM, et al. Fatty acid-binding protein FABP4 mechanistically links obesity with aggressive AML by enhancing aberrant DNA methylation in AML cells. Leukemia. 2016
41. Yan F, Shen N, Pang J, Xie D, Deng B, Molina JR, et al. Restoration of miR-101 suppresses lung tumorigenesis through inhibition of DNMT3a-dependent DNA methylation. Cell death & disease. 2014; 5:e1413. [PubMed: 25210796]
42. Gao XN, Yan F, Lin J, Gao L, Lu XL, Wei SC, et al. AML1/ETO cooperates with HIF1alpha to promote leukemogenesis through DNMT3a transactivation. Leukemia. 2015; 29:1730–1740. [PubMed: 25727291]

Author Manuscript Author Manuscript Author Manuscript Author Manuscript

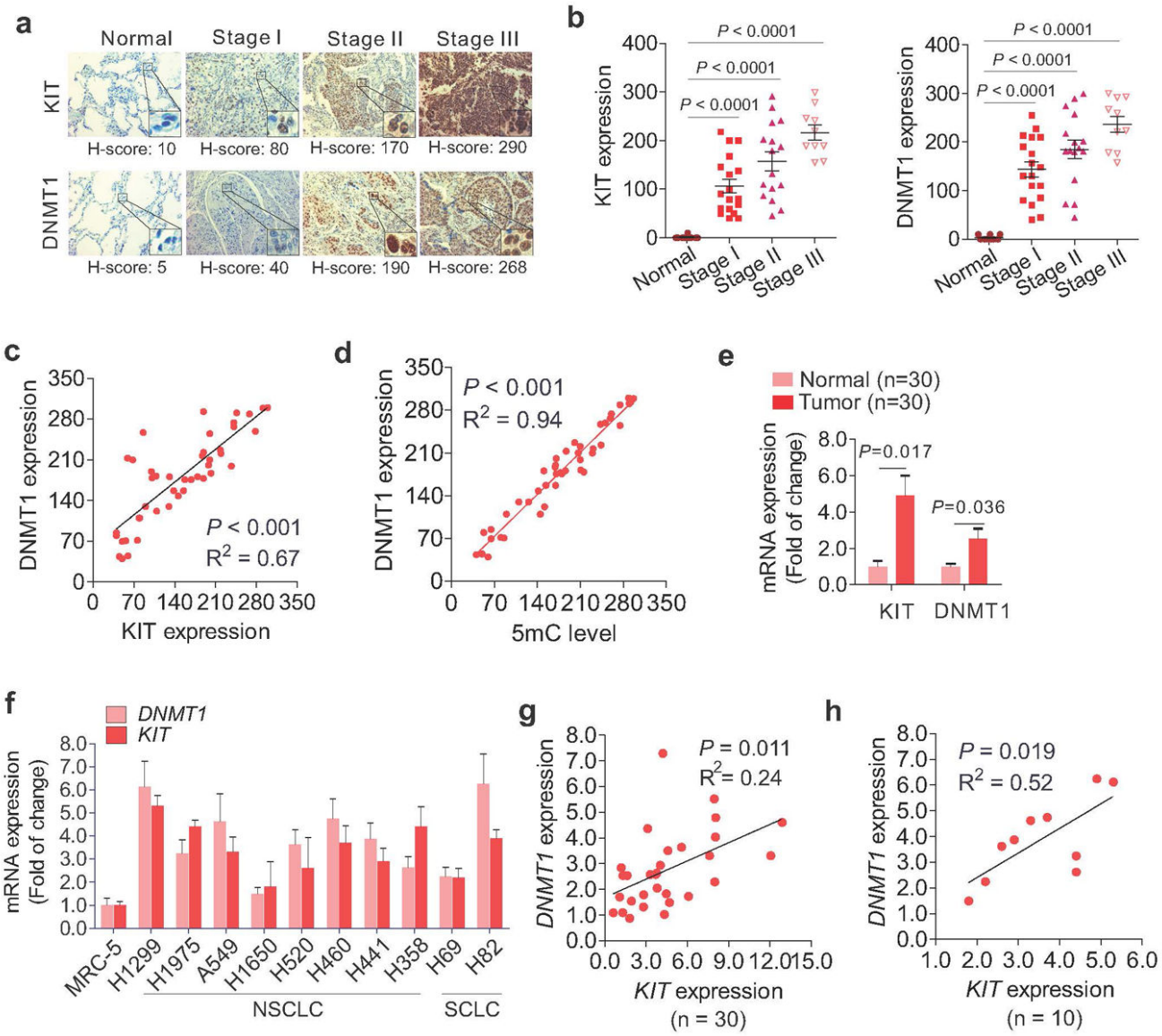

Figure 1.

DNMTs and KIT are frequently overexpressed and positive correlated in lung cancer. (**a**) IHC staining for human NSCLC TMA. Representative micrographs with the H-score for each group are shown (magnification ×200). (**b**) Graph indicates gene expression levels at the different stages of lung cancer. Data were analyzed using one-way ANOVA followed by Dunnett's test; Horizontal bars indicate the mean±SE. (**c**) Scatter plot shows the correlation of KIT with DNMT1. (**d**) Scatter plot shows the correlation of DNMT1 with 5mC. (**e** and **f**) qPCR for the expression of *KIT* and *DNMT1* in fresh-frozen human lung cancer tissues (n=30, **e**) or in human lung cancer cell lines (**f**). (**g**) Scatter plot showing the correlation of *KIT* with *DNMT1* derived from (**e**). (**h**) Scatter plot showing the correlation of *KIT* with *DNMT1* derived from (**f**). Note: In **b**, **c** and **d**, Y- or X-axis represents the H-Score derived from IHC staining in (**a**); In **c**, **d**, **g** and **h**, R: Pearson correlation coefficients; R^2: means

Author Manuscript Author Manuscript Author Manuscript Author Manuscript

"the goodness of fit". Statistical significance was calculated by Pearson correlation coefficients.

Author Manuscript Author Manuscript Author Manuscript Author Manuscript

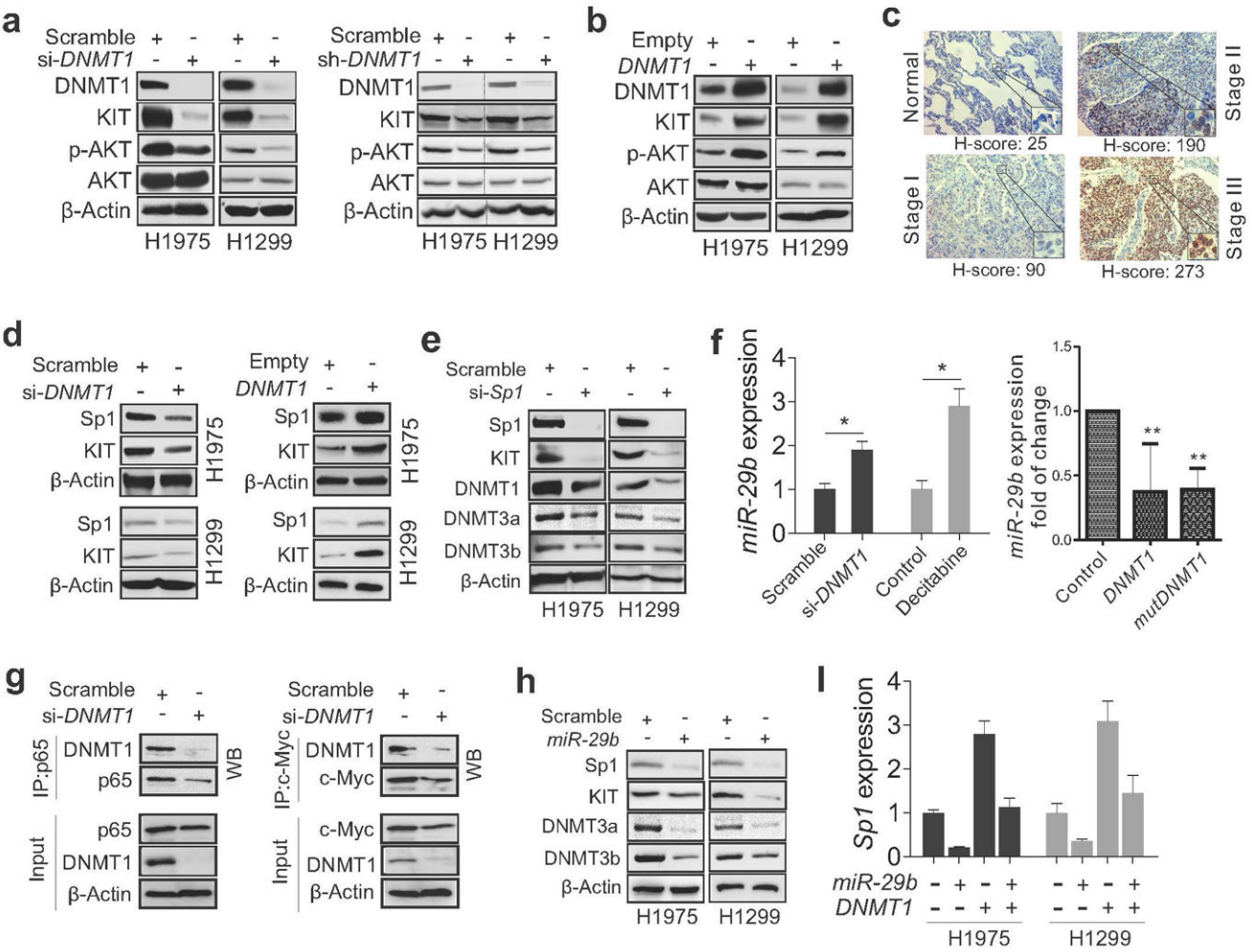

Figure 2.

DNMT1 positively regulates *KIT* expression by Sp1/*miR-29b* network. (**a** and **b**) H1975 and H1299 cells were transfected with *DNMT1* siRNA (a, left), shRNA vectors (**a**, right) or expression plasmids (**b**) for 48 hours and the total cell lysates were subjected to Western blot. (c**)** NSCLC TMA was stained with anti-Sp1. Representative micrographs with the H-score for each group are shown (×200). (**d**) Western blot in H1975 and H1299 cells transfected with *DNMT1* siRNA (left) or expression vector (right) for 48 hours. (**e**) H1975 and H1299 cells were transfected with *Sp1* siRNA and subjected to Western blot. (**f**) qPCR assessing *miR-29b* expression in H1975 and H1299 cells transfected with *DNMT1* siRNA or treated with decitabine (left) or in H1975 cells transfected with *DNMT1* wild-type or mutant expression vectors (right) for 48 hours. **P*<0.05, ***P*<0.01. (**g**) H1975 cells were transfected with *DNMT1* siRNA for 48 hours and subjected to immunoprecipitation followed by Western blot. Input, the whole cell lysates. (**h**) Western blot in H1975 cells transfected with *miR-29b* for 48 hours. (**i**) qPCR to assess Sp1 expression in H1975 and H1299 cells transfected with *DNMT1* expression vector for 24 hours and *miR-29b* for another 24 hours. Note: si, siRNA; sh, shRNA.

Author Manuscript Author Manuscript Author Manuscript Author Manuscript

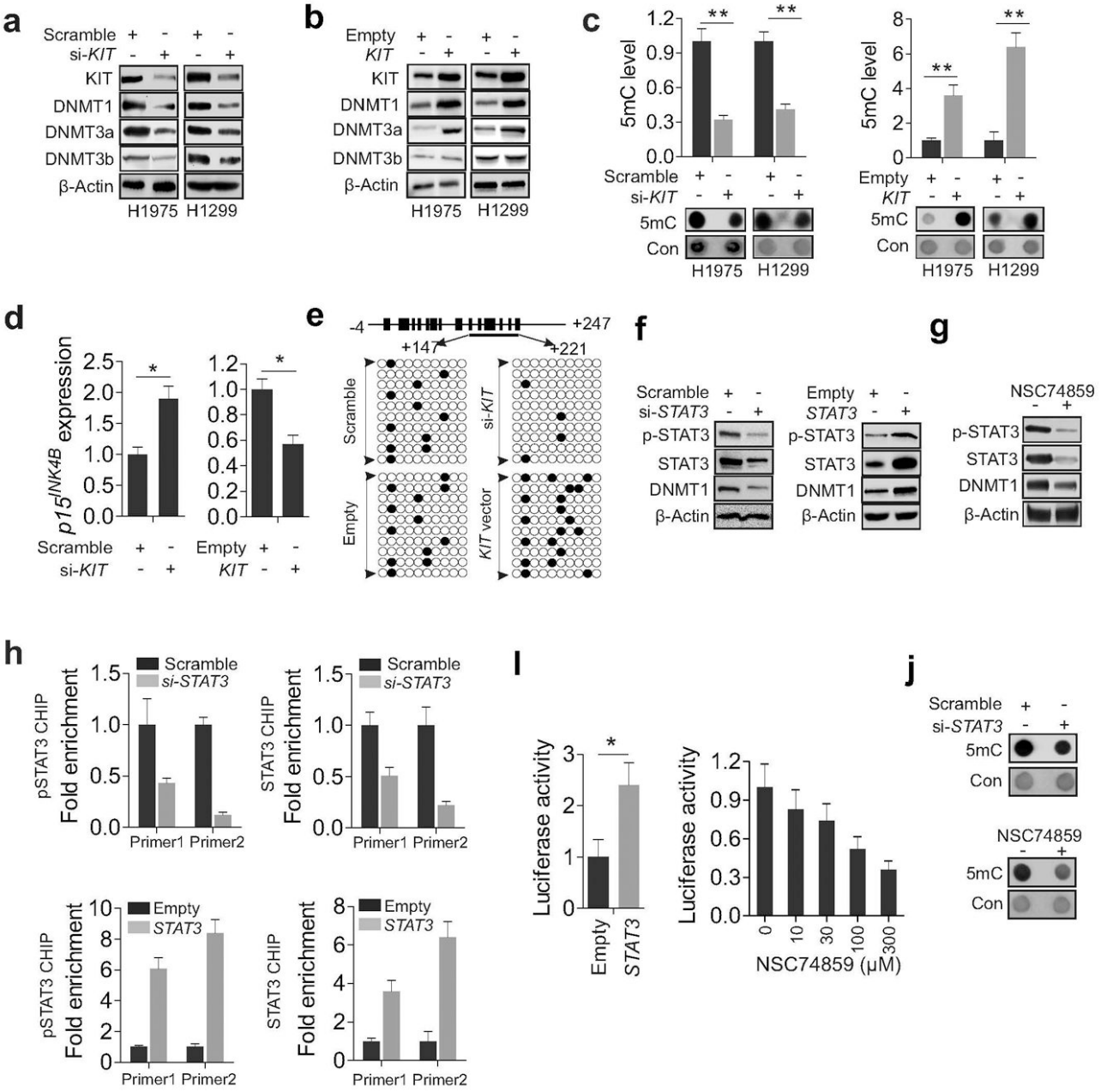

Figure 3.

KIT kinase activity contributes to DNA methylation. (**a** and **b**) H1975 and H1299 cells were transfected with *KIT* siRNA (**a**) or expression vector (**b**) for 48 hours and subjected to Western blot. (**c**) H1975 and H1299 cells were transfected with *KIT* siRNA (left) or expression vectors (right) for 48 hours and the genomic DNA was subjected to Dotblot. ** $P<0.01$. (**d**) qPCR for $p15^{INK4B}$ expression in H1975 cells transfected with *KIT* siRNA (left) or expression vectors (right) for 48 hours. (**e**) Bisulfite sequencing of $p15^{INK4B}$ promoter in H1975 cells transfected with *KIT* siRNA (upper) or expression vectors (lower) for 48 hours. CpG locations are indicated as vertical bars in the promoter and first exon of

Author Manuscript Author Manuscript Author Manuscript Author Manuscript

p15^{INK4B}. Arrows indicate the bisulfite sequencing region (transcription start site +147 to +221). Open circles indicate unmethylated CpG sites, solid circles indicate methylated CpG sites. Results of 10 clones are presented. (**f**) Western blot in H1975 cells transfected with S*TAT3* siRNA (left) or expression vectors (right) for 48 hours. (**g**) H1975 cells were treated with 30 μM NSC74859 for 24 hours and subjected to Western blot. (**h**) ChIP assay in H1975 cells transfected with S*TAT3* siRNA (upper) or expression vector (lower) for 48 hours. The change of STAT3 binding in *DNMT1* promoter was assessed by qPCR. (**i**) left: H1975 cells were transfected with pGL3-*DNMT1* alone or plus *STAT3* vectors for 48 hours; right: H1975 cells were transfected with pGL3-*DNMT1* vector 24 hours and NSC74859 was added for further 24 hours, which was followed by the measurement of luciferase activity. (**j**) Dotblot to measure global DNA methylation in H1975 cells transfected with *STAT3* siRNA (upper) for 48 hours or treated with NSC74859 for 24 hours (lower). Note: pSTAT3, phosphorylated STAT3; si, siRNA; Con, loading control.

Author Manuscript Author Manuscript Author Manuscript Author Manuscript

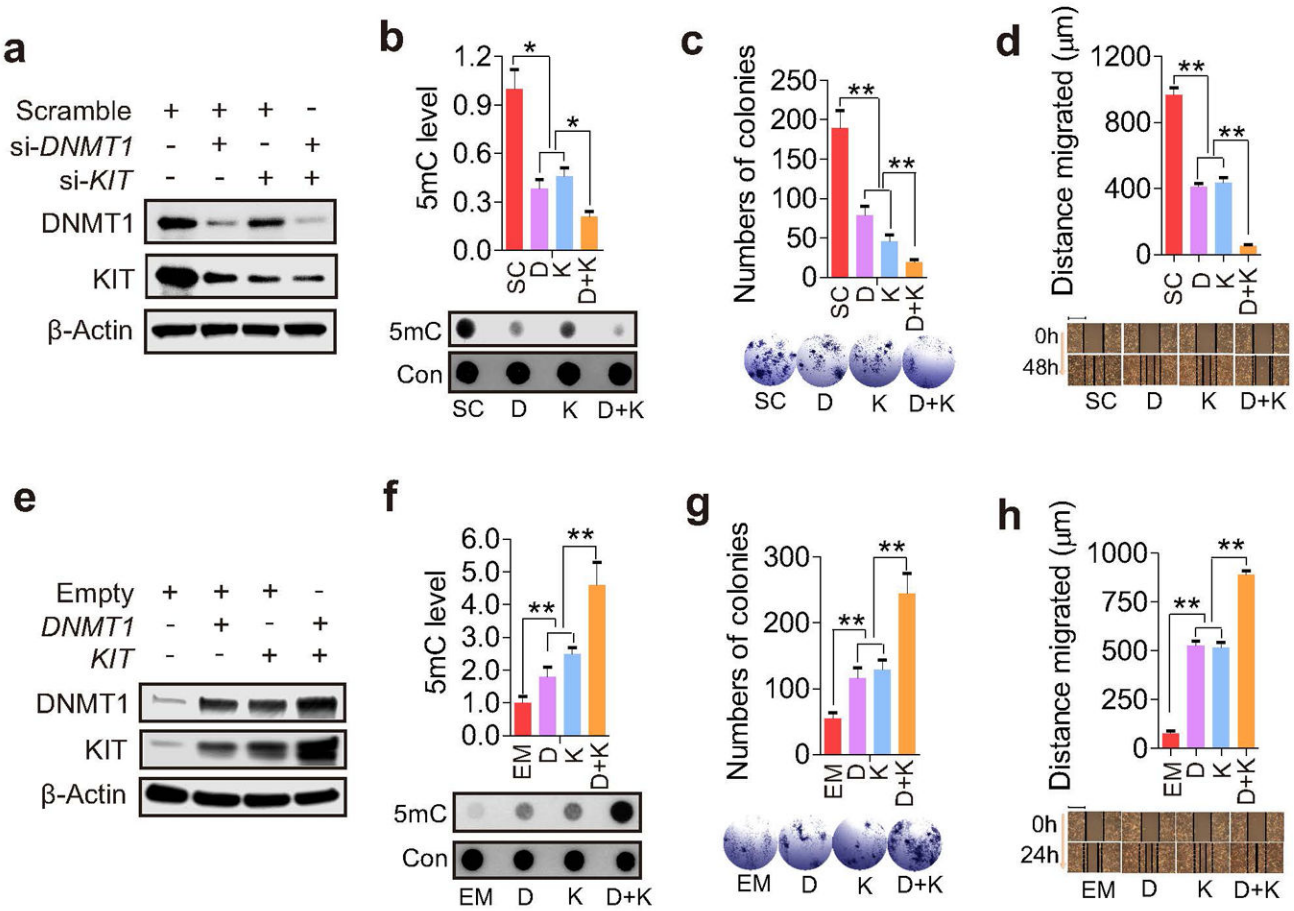

Figure 4.

DNMT1 and KIT cooperatively regulate mobility and aggressiveness of lung cancer cells *in vitro*. **a**–**d**, H1975 cells were transfected with scramble, *DNMT1*, *KIT* or both siRNA, (**a**) Western blot using total protein lysates; (**b**) Representative pictures of Dotblot (lower) and the relative densitometric intensities (upper) using genomic DNA; (**c**) Representative pictures of colony-forming assay (lower) and the quantification of colonies (upper); (**d**) Representative pictures of wound-healing assay (lower) and the quantification of distance migrated (upper). **e**–**h**, H1975 cells were transfected with empty, *KIT*, *DNMT1* or both expression vectors, (**e**) Western blot; (**f**) Representative pictures of Dotblot (lower) and the relative densitometric intensities (upper); (**g**) Representative pictures of colony-forming assay (lower) and the quantification of colonies (upper); (**h**) Representative pictures of wound-healing assay (lower) and the quantification of distance migrated (upper). Error bars represent SD. *P<0.05; **P<0.01. In **b** to **d**, **f** to **h**, the abbreviations of SC, EM, D, K and D+K are scramble, empty, *DNMT1*, *KIT* and *DNMT1*+*KIT*; Con, loading control; **d** and **h**, scale bars, 1 mm.

Author Manuscript Author Manuscript Author Manuscript Author Manuscript

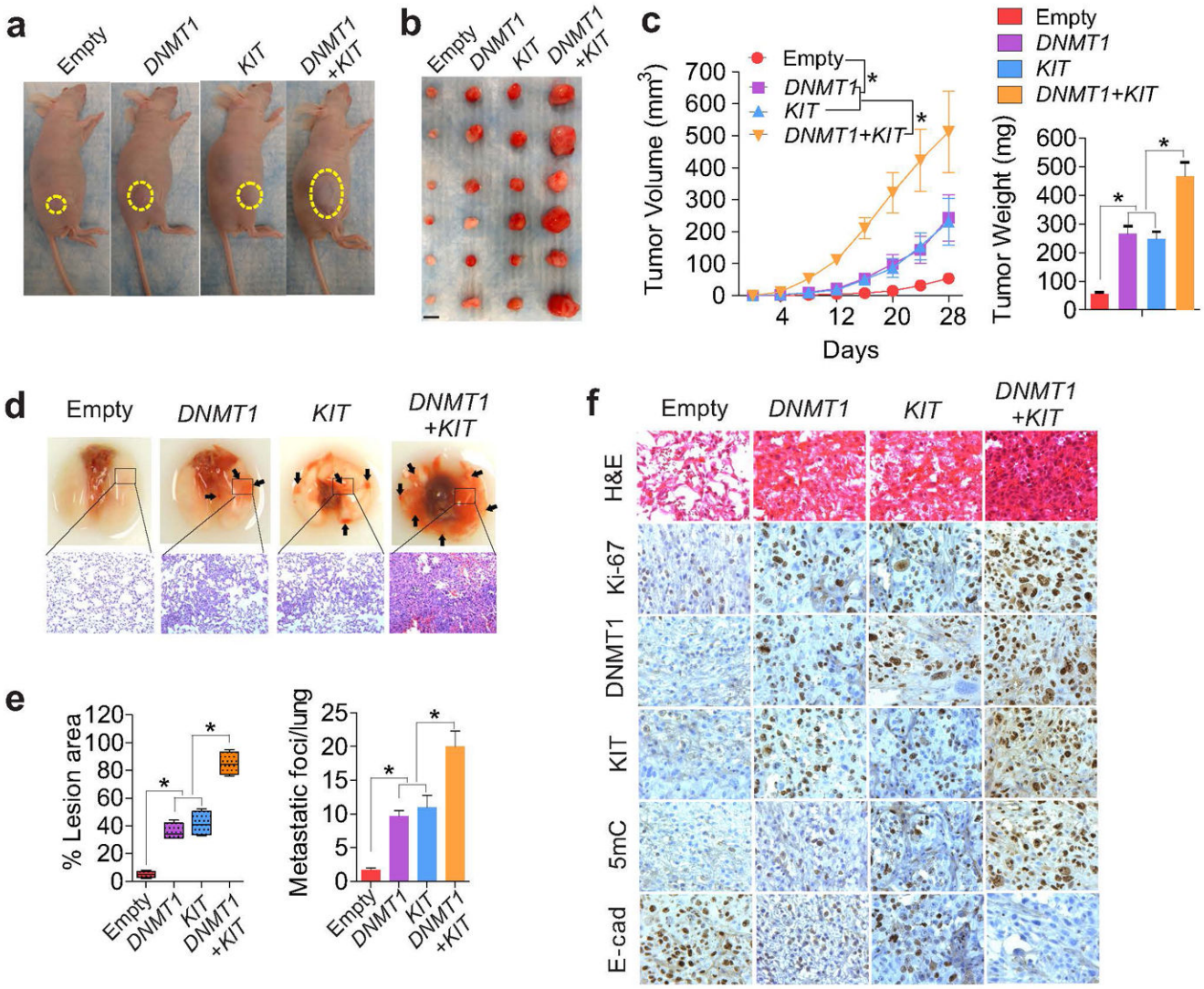

Figure 5.

Co-overexpression of *DNMT1* and *KIT* confers enhanced tumorigenicity. (**a**) H1975 cells were transfected with empty, *DNMT1*, *KIT*, or both expression vectors. At 6 hours after transfection, the transfected cells (1×10^6) were subcutaneously injected into nude mice (n=6 tumors/group). Pictured are the representative external views of tumor-bearing nude mice at day 28 after implantation. (**b**) Pictured are the tumors dissected at day 28 after implantation. Total 6 tumors from each group are shown. Scale bar, 5mm. (**c**) The graph represents the mean tumor volume at the indicated days during the experiment (left). The tumor weight graphs derived from nude mice injected with transfected H1975 cells (right), n=6 tumors/group. (**d**) Representative images of lungs and H&E staining for boxed lesion. Arrows indicate focal tumor nodules on lung surfaces (n=3 mice/group). (**e**) The quantification of lesion area (left) and tumor nodules (right) from lungs (n=3 mice/group). (**f**) Representative H&E or IHC staining of tumor sections from tumor-bearing nude mice. Note: For **c** and **e**, values represent the mean+SD. *P<0.05.

Author Manuscript Author Manuscript Author Manuscript Author Manuscript

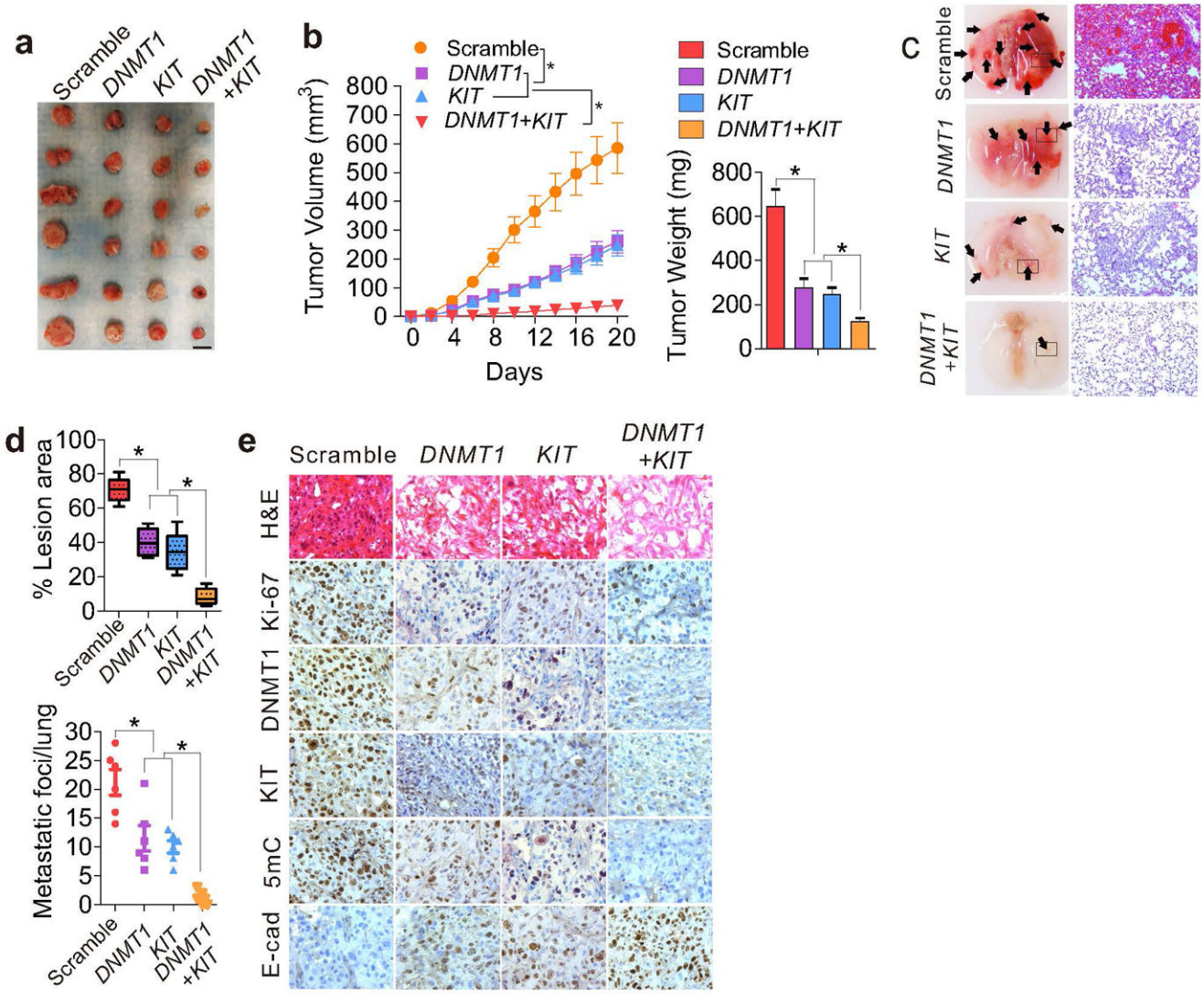

Figure 6.

Co-depletion of *KIT* and *DNMT1* synergistically contributes to *in vivo* reduced tumorigenic potential and metastatic ability. (**a**) LL/2 cells were transfected with scramble, *DNMT1*, *KIT* and both siRNA. At 6 hours after transfection, the transfected cells (0.5×10^6) were subcutaneously injected into the C57BL/6 mice. The photographs of tumors derived from transfected LL/2 cells and dissected at day 20 after implantation (n=6 tumors/group). Scale bar, 5mm. (**b**) Growth curves (left) and weight graph (right) of tumors derived from the indicated gene types, n=6 tumors/group. Error bars represent SD. *P<0.05. (**c**) left: representative images of lung from mice injected with transfected LL/2 cells. Arrows indicate focal tumor nodules on the lung surfaces; right: H&E staining images of lung sections. The boxed regions are magnified (×200) and shown beside, n=6 mice/group. (**d**) Graphs show the quantification of lesion area (upper) and metastatic foci (lower) in the

different group of treatments reported in (**c**). Horizontal bars indicate the mean±SD. (**e**) representative H&E or IHC staining of tumor sections.

Author Manuscript Author Manuscript Author Manuscript Author Manuscript